NJC

PAPER

View Article Online
View Journal | View Issue

Cite this: *New J. Chem.*, 2015, 39, 7617

Investigation of the "bent sandwich-like" divalent lanthanide hydro-tris(pyrazolyl)borates $Ln(Tp^{iPr2})_2$ (Ln = Sm, Eu, Tm, Yb)†‡

Marcel Kühling,[a] Claudia Wickleder,*[b] Michael J. Ferguson,[c] Cristian G. Hrib,[a] Robert McDonald,[c] Markus Suta,[b] Liane Hilfert,[a] Josef Takats*[c] and Frank T. Edelmann*[a]

Received (in Montpellier, France) 6th March 2015,
Accepted 5th May 2015

DOI: 10.1039/c5nj00568j

www.rsc.org/njc

The series of homoleptic lanthanide(II) "bent sandwich-like" hydro-tris(pyrazolyl)borate complexes $Ln(Tp^{iPr2})_2$ (Ln = Sm (**1**), Eu (**2**), Tm (**3**), Yb (**4**); Tp^{iPr2} = hydro-tris(3,5-diisopropylpyrazolyl)borate) has been completed by the synthesis of the hitherto unknown europium and ytterbium derivatives **2** and **4**. Both compounds were prepared in high yields by treatment of $LnI_2(THF)_2$ (Ln = Eu, Yb) with 2 equiv. of KTp^{iPr2} in a THF solution. Although the molecules are sterically highly congested, an X-ray diffraction study of bright red **4** revealed a similar bent B–Yb–B arrangement (151.1° and 153.9°, two independent molecules) as in the previously investigated Sm(II) and Tm(II) complexes **1** and **3**. An initial reactivity study showed a very different behavior with acetonitrile. While **2** and **4** proved to be unreactive toward acetonitrile, the more strongly reducing Sm(II) complex **1** yielded two new products. The major product was the dark green-black acetonitrile solvate $Sm^{II}(Tp^{iPr2})_2{\cdot}CH_3CN$ (**5**), while the second product, the colorless $(Tp^{iPr2})Sm^{III}(3,5\text{-}{}^iPr_2pz)_2(NCCH_3)$ (**6**) with two 3,5-diisopropyl-pyrazolate ligands, resulted from oxidation of samarium to the trivalent state and degradation of a Tp^{iPr2} ligand. Disappointingly, from the most reducing Tm(II) complex **3** only the ligand fragmentation product pyrazabole, $[HB(3,5\text{-}{}^iPr_2pz)_2]_2$ (**7**), could be isolated and the fate of the Tm containing by-product(s) remains unknown. The new compounds **4–6** were structurally authenticated through single-crystal X-ray diffraction. The europium compound **2** shows an extremely bright yellow emission in solution, which can be observed also at daylight excitation, as well as in the solid state. The high intensity is even remarkable when compared to other Eu(II) containing materials. The photoluminescence was investigated with the conclusion that the rigidity of this complex is responsible for these outstanding luminescence properties.

1. Introduction

The discovery of the divalent lanthanide sandwich complexes $Ln(C_5Me_5)_2$ (Ln = Sm, Eu, Yb; C_5Me_5 = η^5-pentamethylcyclopentadienyl) *ca.* 30 years ago sparked a firework of unprecedented reactivity and structures in organolanthanide chemistry.[1,2] The exceptionally high reactivity of decamethylsamarocene, $Sm(C_5Me_5)_2$, even allowed the isolation of the first dinitrogen complex of an f-element, $(\mu\text{-}N_2)[Sm(C_5Me_5)_2]_2$,[3] and still today novel reactions of decamethylsamarocene are being uncovered.[4] A fascinating structural feature of the unsolvated lanthanide sandwich complexes $Ln(C_5Me_5)_2$ (Ln = Sm, Eu, Yb) is their bent metallocene structure in the solid state. This opens up the coordination sphere of the central lanthanide(II) ions and accounts for the high reactivity of these compounds. Various theoretical and spectroscopic studies have been carried out to fully understand the nature of this unexpected deviation from the normal linear sandwich structure (Scheme 1(a)). It is now generally accepted, based on computational studies, that the unusual bent sandwich structure of $Ln(C_5Me_5)_2$ (Ln = Sm, Eu, Yb) is the result of attractive dispersion/van der Waals interactions.[5]

Trofimenko's hydro-tris(pyrazolyl)borate ligands ("scorpionates") have proven to be useful alternatives to the omnipresent cyclopentadienyl ligands.[6,7] Like the cyclopentadienyls, these tridentate, monoanionic ligands can also be greatly varied in their steric bulk

[a] *Chemisches Institut der Otto-von-Guericke-Universität Magdeburg, Universitätsplatz 2, 39106 Magdeburg, Germany. E-mail: frank.edelmann@ovgu.de; Fax: +49 391 671-2933; Tel: +49 391 675-8327*
[b] *Universität Siegen, Anorganische Chemie, Adolf-Reichwein-Straße, 57068 Siegen, Germany. E-mail: wickleder@chemie.uni-siegen.de; Fax: +49 271 740-2555; Tel: +49 271 740-4217*
[c] *Department of Chemistry, University of Alberta, Edmonton, Alberta, AB, Canada T6G 2G2. E-mail: joe.takats@ualberta.ca; Fax: +001 780 492-8231; Tel: +001 780 492-4944*

† Dedicated to the memory of Professor Michael F. Lappert, a pioneer of organometallic chemistry.

‡ Electronic supplementary information (ESI) available. CCDC 1051399–1051401. For ESI and crystallographic data in CIF or other electronic format see DOI: 10.1039/c5nj00568j

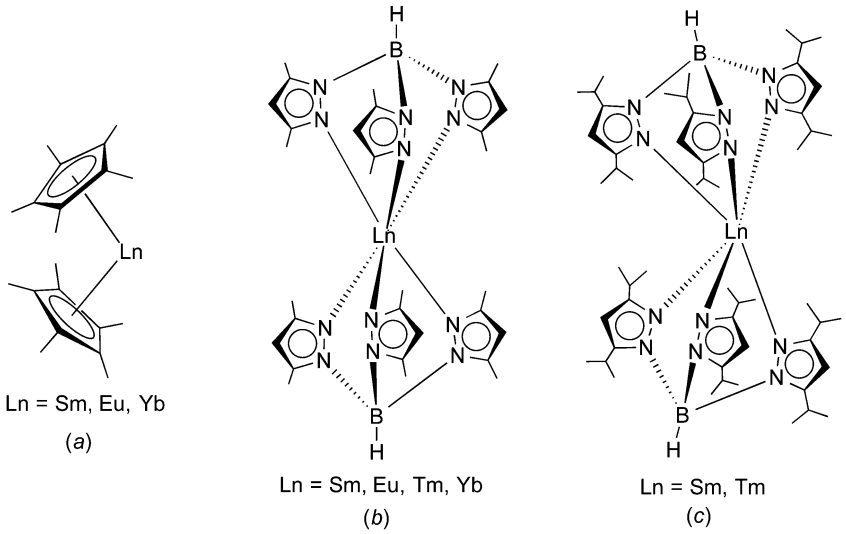

Scheme 1 Comparison of the molecular structures of (a) $Ln(C_5Me_5)_2$ (Ln = Sm, Eu, Yb),[1,2] (b) $Ln(Tp^{Me_2})_2$ (Ln = Sm, Eu, Tm, Yb),[8–11] and (c) $Ln(Tp^{iPr_2})_2$ (Ln = Sm (**1**), Tm(**3**)).[14]

by changing the substituents in the 3- and 5-positions of the pyrazolyl rings. According to Trofimenko's nomenclature, the abbreviation Tp stands for the ring-unsubstituted hydro-tris-(pyrazolyl)borate, whereas *e.g.* Tp^{Me_2} denotes the sterically more demanding hydro-tris(3,5-dimethylpyrazolyl)borate. The homoleptic divalent lanthanide complexes $Ln(Tp^{Me_2})_2$ (Ln = Sm, Eu, Yb) have been found to adopt a highly symmetrical, trigonal antiprismatic molecular structure comprising a linear B···Ln···B arrangement (Scheme 1(b)).[8–11] Apparently, this "sandwich-like" structure of $Ln(Tp^{Me_2})_2$ is the result of the much larger cone angle of Tp^{Me_2} (239°) as compared to the C_5Me_5 ligand with 142°.[12] Most recently, these studies have been extended to the even larger hydro-tris-(3,5-diisopropylpyrazolyl)borate ligand (Tp^{iPr_2}).[13] It was possible to isolate homoleptic complexes of this ligand with divalent samarium and thulium.[14] Rather surprisingly, crystal structure determinations revealed a "bent sandwich-like" molecular structure like $Ln(C_5Me_5)_2$ as shown in Scheme 1(c). Computational studies indicated that steric repulsion between the isopropyl groups forces the Tp^{iPr_2} ligands apart and permits the formation of unusual interligand C–H···N hydrogen-bonding interactions that help stabilizing the structure.[14]

Among the "classical" divalent lanthanide ions (Sm^{2+}, Eu^{2+}, Yb^{2+}) only the homoleptic samarium(II) Tp^{iPr_2} complex $Sm(Tp^{iPr_2})_2$ (**1**) has previously been prepared and fully characterized.[14] In this article we report the synthesis and characterization of the corresponding divalent europium and ytterbium species $Eu(Tp^{iPr_2})_2$ (**2**) and $Yb(Tp^{iPr_2})_2$ (**3**) as well as the behavior of the full series of $Ln(Tp^{iPr_2})_2$ complexes toward acetonitrile, and the first results on the photoluminescence of compound **2**.

2. Results and discussion

2.1 Synthesis and reactivity

The title compounds were prepared following the synthetic route outlined in Scheme 2. Similar to the recently reported preparation of the samarium(II) and thulium(II) derivatives **1** and **3**,[14] reactions of $EuI_2(THF)_2$ and $YbI_2(THF)_2$ with 2 equiv. of KTp^{iPr_2} were carried out in THF solutions at room temperature.

Both reactions were accompanied by striking color changes to "neon-yellow" (Eu) or bright red (Yb), respectively, and formation of a white precipitate (KI). After removal of the potassium iodide by-product through filtration, the products could be readily extracted with *n*-pentane. Recrystallization from very concentrated solutions in *n*-pentane at −20 °C for 24 h afforded yellow $Eu(Tp^{iPr_2})_2$ (**2**) and bright red $Yb(Tp^{iPr_2})_2$ (**4**) in high yields (**2**: 83%, **4**: 77%). Both new compounds were fully characterized by the usual combination of spectroscopic data and elemental analyses. While the ^1H NMR spectrum of diamagnetic **4** showed the expected number of resonances for the Tp^{iPr_2} ligands, meaningful ^1H and ^{13}C NMR data for paramagnetic **2** could not be obtained, as noted also for $Eu(C_5Me_5)_2$ and its derivatives,[2e,h] and $Eu(Tp^{Me_2,Et})_2$.[10] In both cases, the ^{11}B NMR spectra showed a single broad resonance (**2**: $\delta = -7$ ppm (very broad), **4**: $\delta = -6.2$ ppm). Moreover, $Yb(Tp^{iPr_2})_2$ (**4**) was characterized by its ^{171}Yb NMR spectrum. High-resolution ^{171}Yb NMR spectroscopy is well established as a valuable tool for characterizing divalent (diamagnetic) ytterbium complexes in solution and in the solid state.[15,16] ^{171}Yb resonances have been reported to encompass a chemical shift dispersion of some 3000 ppm (from *ca.* δ +2500 to −500 ppm).[15c] The ^{171}Yb spectrum of **4** comprises a singlet at $\delta = 619.1$ ppm. An almost identical value ($\delta = 614$ ppm) has previously been reported for the ytterbium(II) bis(trimethylsilyl)amide complex $Yb[N(SiMe_3)_2]_2(OEt_2)_2$.[15a]

The recent structural characterization of **1** and its thulium congener **3** had already shown that these "bent sandwich-like" molecules are sterically highly congested. Thus for an initial reactivity study, the reagent acetonitrile was chosen in order to find out if a small, rod-like molecule such as CH_3CN could enter the coordination sphere and bind to the central Ln^{2+} ions in **1–4**. Surprisingly, no reaction with acetonitrile was observed

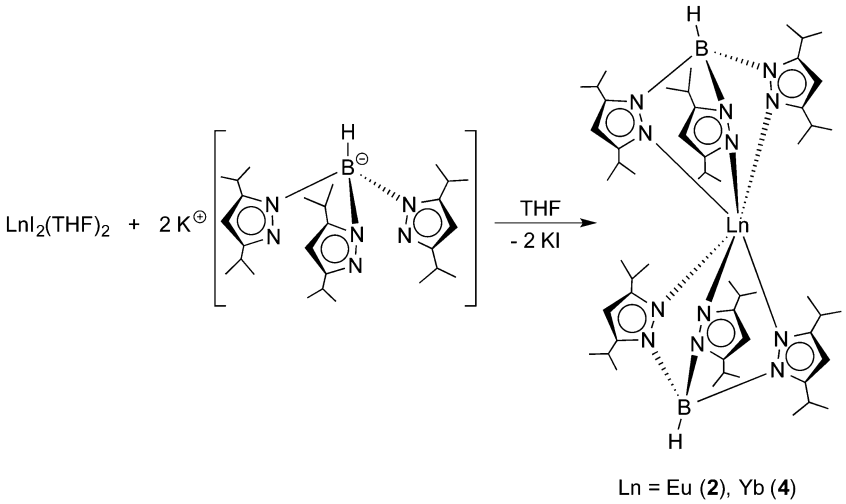

Scheme 2 Synthesis of $Ln(Tp^{iPr_2})_2$ (Ln = Eu (**2**), Yb (**4**)).

for the europium and ytterbium complexes **2** and **4** even upon slight warming. Both complexes produced clear solutions in dry acetonitrile, from which they could be recovered unchanged by evaporation or cooling. In fact, acetonitrile appears to be a suitable solvent for recrystallizing bulk samples of **2** and **4**. This is not the case for the Sm(II) and Tm(II) complexes **1** and **3**. Unexpectedly, and curiously the Sm(II) complex is virtually insoluble in acetonitrile. Addition of acetonitrile to solid **1** produces an almost colorless supernatant and a very dark green, almost black solid. The latter was shown to be unchanged $Sm(Tp^{iPr_2})_2$ by ^{1}H NMR spectroscopy. To study the behavior of $Sm(Tp^{iPr_2})_2$ toward acetonitrile, acetonitrile was added to a dark green solution of **1** in diethyl ether. Concentration of the solution by slow evaporation at RT in the dry-box resulted in the formation of two types of crystals, dark green and colorless; the former was shown to be $Sm^{II}(Tp^{iPr_2})_2{\cdot}CH_3CN$ (**5**), with a solvate molecule of CH_3CN in the lattice, while the latter proved to be the partially ligand fragmented Sm(III) complex, (Tp^{iPr_2})-$Sm^{III}(3,5\text{-}^iPr_2pz)_2(NCCH_3)$ (**6**), with a coordinated $NCCH_3$ ligand. The most reducing Tm(II) complex **3** dissolved in acetonitrile and gave a dark, plum-red solution which slowly bleached with time, indicating oxidation of Tm(II) to Tm(III). Multiple attempts to grow crystals from various solvent mixtures only resulted in the formation of colorless blocks which were shown, by X-ray diffraction,

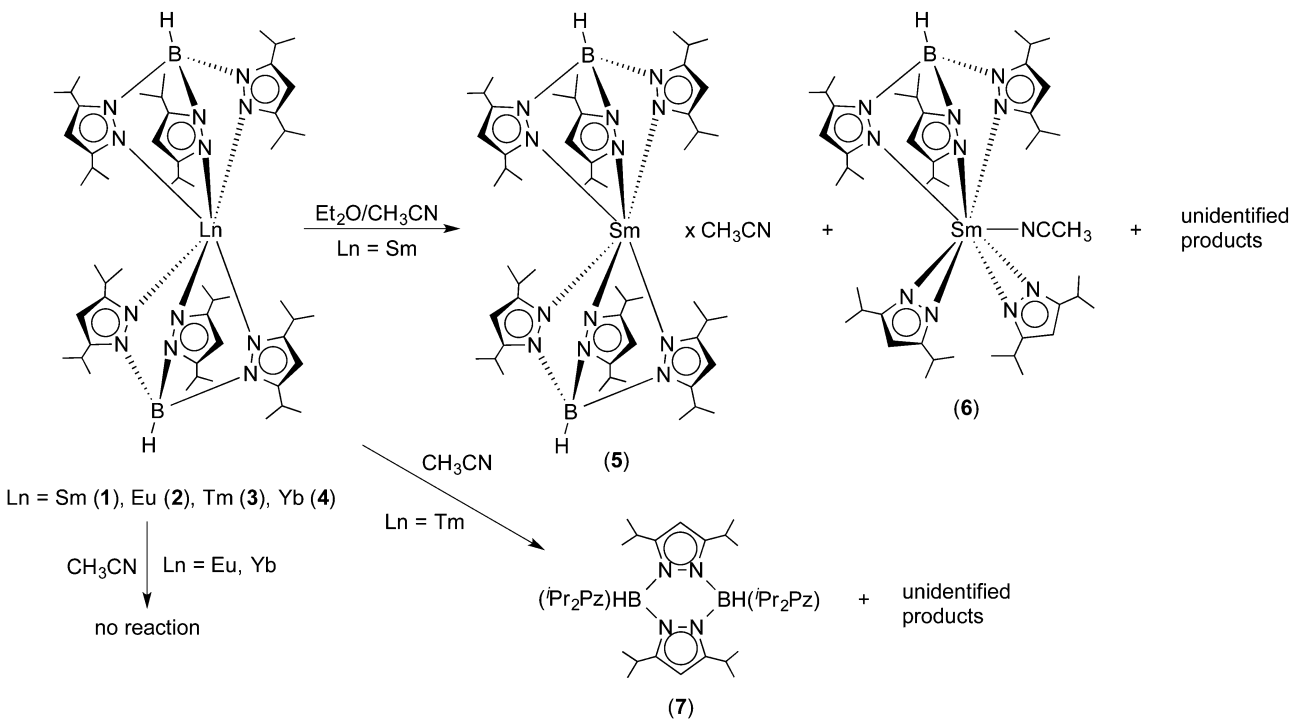

Scheme 3 Reactivity of $Ln(Tp^{iPr_2})_2$ (Ln = Sm (**1**), Eu (**2**), Tm (**3**), Yb (**4**)) toward acetonitrile.

to be the pyrazabole derivative $[HB(3,5\text{-}^{i}Pr_2pz)]_2$ (**7**). No thulium-containing product could be isolated. Scheme 3 summarizes the results of this initial reactivity study of **1–4** toward acetonitrile.

2.2 X-ray crystallography

The new compounds **4–6** were structurally authenticated through single-crystal X-ray diffraction. Bright red X-ray quality single-crystals of **4** were obtained by cooling a very concentrated solution in *n*-pentane to −20 °C, whereas single crystals of both **5** (green) and **6** (colorless) were obtained from the reaction of **1** with acetonitrile in diethyl ether according to Scheme 3. The single-crystals of **4** were found to contain one molecule of *n*-pentane per formula unit. Crystallographic data of **4–6** are listed in Table 1. The molecular structure of the Yb complex, with numbering scheme, is shown in Fig. 1. Just like the Sm and Tm compounds **1** and **3**, the ytterbium(II) complex $Yb(Tp^{iPr_2})_2$ also exhibits the "bent sandwich-like" geometry, and indeed the compound is isomorphous with the Tm analogue and contains two independent molecules per asymmetric unit. The B–Yb–N angles in the two independent molecules are 151.1° and 153.9°, respectively. This can be favorably compared to the B–Ln–B angles of 150.1° in the samarium(II) analogue **1** and 152.2° in $Tm(Tp^{iPr_2})_2$ (**3**).[14] As expected from the nearly identically sized Yb(II) and Tm(II) ions,[17] the Ln–N distances in **3** and **4** are nearly identical and the bond angles and torsional angles are similar as well (*cf.* Table S1 in the ESI‡).

The structure of the Sm(II) compound $Sm^{II}(Tp^{iPr_2})_2{\cdot}CH_3CN$ (**5**), obtained by crystallization from CH_3CN/Et_2O, is shown in Fig. 2, and Fig. 3 shows the packing diagram. The lattice acetonitrile is just a solvate as the distance between Sm and N1S is over 6 Å, thus there is no bonding contact between Sm and $NCCH_3$ molecule. As opposed to the crystals obtained from pentane, in this case there is only one molecule per asymmetric unit. Nevertheless, the geometry is still "bent sandwich-like" and the B1–Sm–B2 angle of 151.19(5)° is very similar to the 150.1° in the previously reported structure of $Sm^{II}(Tp^{iPr_2})_2$,[14] demonstrating once again that the bent geometry is an inherent molecular feature of all divalent $Ln(Tp^{iPr_2})_2$ complexes and is not due to crystal packing effects. However, the latter may have some subtle effect since the Sm–N32 distance of 2.735(2) Å is longer that the 2.655(6) Å seen before and the torsion angle of this pyrazolyl moiety is also large, Sm–N32–N31–B1 = 62.4(2)°, as opposed to the 20° average observed before.[14]

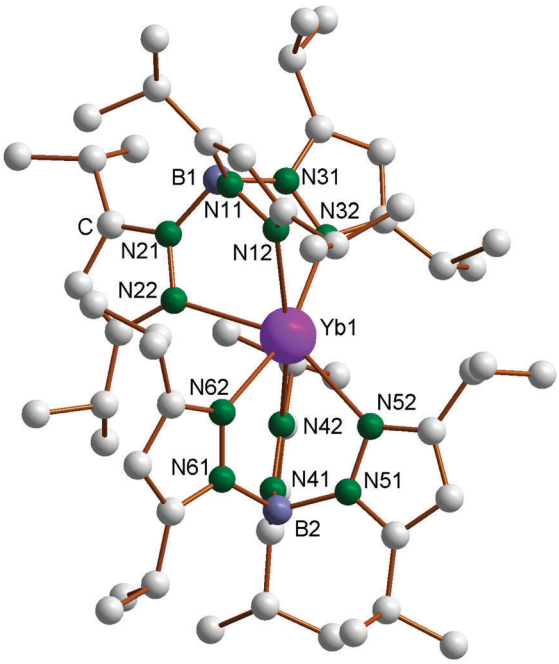

Fig. 1 Molecular structure of $Yb(Tp^{iPr_2})_2$ (**4**). Selected bond lengths (Å) and angles (°), molecule 1: Yb1–N12 2.528(2), Yb1–N22 2.530(2), Yb1–N32 2.550(2), Yb1–N42 2.487(2), Yb1–N52 2.589(2), Yb1–N62 2.478(2), B1–Yb1–B2 151.1. Molecule 2: Yb2–N12′ 2.525(2), Yb2–N22′ 2.522(2), Yb2–N32′ 2.528(2), Yb2–N42′ 2.498(2), Yb2–N52′ 2.540(2), Yb2–N62′ 2.502(2), B3–Yb2–B4 153.9.

The molecular structure of the oxidized product $(Tp^{iPr_2})Sm(3,5\text{-}^{i}Pr_2Pz)_2(NCCH_3)$ (**6**) is shown in Fig. 4, with important bond distances and angles also listed in the figure caption.

Table 1 Crystallographic data for **4–6**

	4	**5**	**6**
Empirical formula	$C_{59}H_{104}B_2N_{12}Yb$	$C_{56}H_{95}B_2N_{13}Sm$	$C_{47}H_{79}BN_{11}Sm$
a (Å)	13.44670 (10)	12.9942 (10)	13.9188 (9)
b (Å)	20.6731 (2)	13.6332 (10)	16.8238 (11)
c (Å)	25.1841 (2)	20.9744 (16)	21.9614 (15)
α (°)	83.2050 (10)	104.2666 (8)	90
β (°)	74.7430 (10)	94.8690 (8)	90.3416 (10)
γ (°)	77.6100 (10)	115.6405 (7)	90
V (Å^3)	6582.53 (10)	3167.5 (4)	5142.5 (6)
Z	4	2	4
Formula weight	1176.20	1122.41	959.37
Space group	$P\bar{1}$	$P\bar{1}$	$P2_1/n$
T (°C)	−173	−100	−80
λ (Å)	0.71073	0.71073	0.71073
D_{calcd} (g cm^{-3})	1.187	1.177	1.239
μ (mm^{-1})	1.464	0.971	1.183
Data/restraints/parameters	39 188/0/1345	14 330/0/658	12 276/0/542
Goodness-of-fit on F^2	1.028	1.051	1.024
R (F_o or F_o^2)	0.0363	0.0271	0.0287
R_w (F_o or F_o^2)	0.0689	0.0678	0.0715

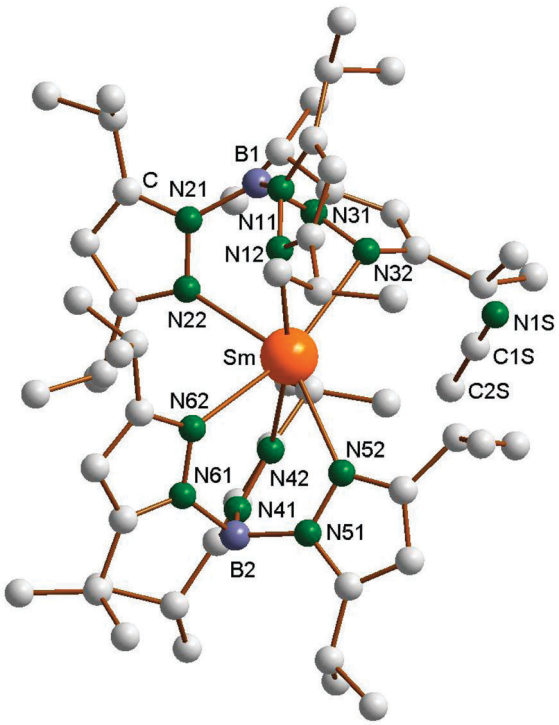

Fig. 2 Molecular structure of $Sm^{II}(Tp^{iPr_2})_2{\cdot}CH_3CN$ (**5**). Selected bond lengths (Å) and angle (°): Sm–N12 2.642(2), Sm–N22 2.638(2), Sm–N32 2.735(2), Sm–N42 2.631(2), Sm–N52 2.634(2), Sm–N62 2.661(2), B1–Sm–B2 151.2.

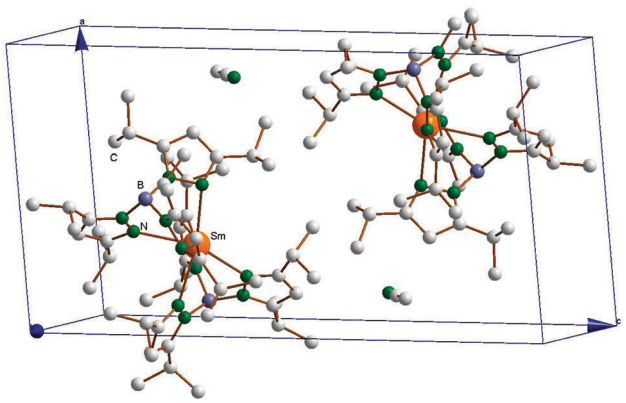

Fig. 3 Crystal packing diagram of $Sm^{II}(Tp^{iPr_2})_2{\cdot}CH_3CN$ (**5**).

The coordination sphere of the Sm(III) center is defined by a classical κ^3-Tp^{iPr_2} ligand, two almost symmetrically bonded κ^2-pyrazolides and N1-bound acetonitrile. The coordination geometry can be roughly described as distorted octahedral, with N12, N22 and mid-points of N41N42 and N51N52 occupying the equatorial and N32 and N1 the axial positions (N32–Sm–N1 = 143.20(6)°). As expected, the Sm–N distances to the anionic κ^2-pyrazolides (2.40 Å ave) are shorter than those to the κ^3-Tp^{iPr_2} ligand (2.560 Å ave), which in turn is shorter than the Sm–$NCCH_3$ distance of 2.601 Å. The Sm–N(Tp^{iPr_2}) distances are shorter than those in $Sm(Tp^{iPr_2})_2$ (**1**), reflecting the smaller size of Sm(III) compared to Sm(II) and also the more congested nature of the latter complex. That sterics still have an influence on the arrangement of the ligands in complex **6** is shown by the less than 180° of the Sm–N1–C1 angle (159.2(2)°), the bending being away from the ^{i}Pr substituent of the two κ^2-pyrazolide ligands.

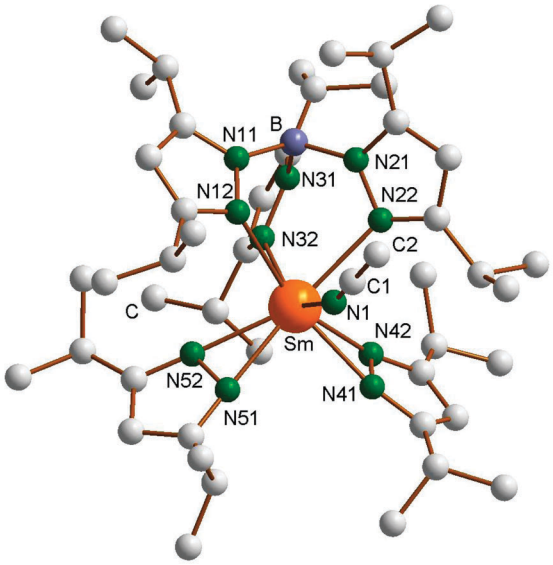

Fig. 4 Molecular structure of $(Tp^{iPr_2})Sm^{III}(3,5\text{-}^iPr_2pz)_2(NCCH_3)$ (**6**). Selected bond lengths (Å) and angles (°): Sm–N1 2.601(2), Sm–N12 2.574(2), Sm–N22 2.571(2), Sm–N32 2.536(2), Sm–N41 2.379(2), Sm–N42 2.420(2), Sm–N51 2.384(2), Sm–N52 2.409(2), N1–Sm–N32 143.20(6), Sm–N1–C1 159.2(2).

2.3 Luminescence study of $Eu(Tp^{iPr_2})_2$ (2)

In general, the luminescence behaviour of divalent lanthanides is very different compared to that of the trivalent ones due to two main reasons. On the one hand, the position of the excited $4f^{n-1}5d^1$ states relative to the $4f^n$ ground state is strongly influenced by the environment and, thus, variable over a wide spectral range. On the other hand, the respective $4f^n \leftrightarrow 4f^{n-1}5d^1$ transitions are parity allowed leading to an intense emission in the most cases.[18] Due to these advantages the most stable divalent ion, Eu^{2+}, is mostly used in modern materials for applications, like LED phosphors, displays and medical markers.[19] While the luminescence properties of Eu^{2+} ions doped in ionic compounds, especially the structure–luminescence-relationship, is well investigated,[20] such investigations of molecular complexes are rather scarce. A notable example is the strong luminescence exhibited by $Eu(Cp^{BIG})_2$ (Cp^{BIG} = $C_5(C_6H_4{}^nBu\text{-}4)_5$).[21] In this contribution we present first results on the photoluminescence behavior of compound **2**. It was found that $Eu(Tp^{iPr_2})_2$ (**2**) shows extremely bright yellowish-green luminescence upon UV irradiation at room temperature in the solid state as well as in *n*-pentane solution, which can be also observed by daylight-excitation (Fig. 5). Fig. 6 shows the luminescence of solid **2** under UV light.

The photoluminescence emission and excitation spectra of this compound are depicted in Fig. 7. The shape and position are typical for Eu(II) photoluminescence, so that it is obvious that Eu^{2+} is the only emitting species. The broad (FWHM = 2245 cm^{-1}) slightly asymmetric emission band

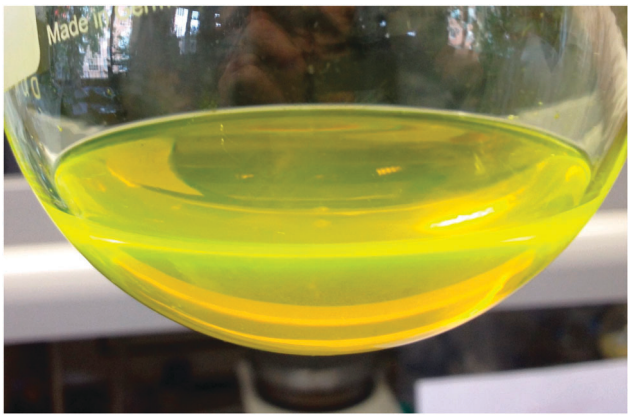

Fig. 5 Bright yellow luminescence of Eu(Tp^{iPr_2})$_2$ (**2**) in *n*-pentane solution excited by daylight.

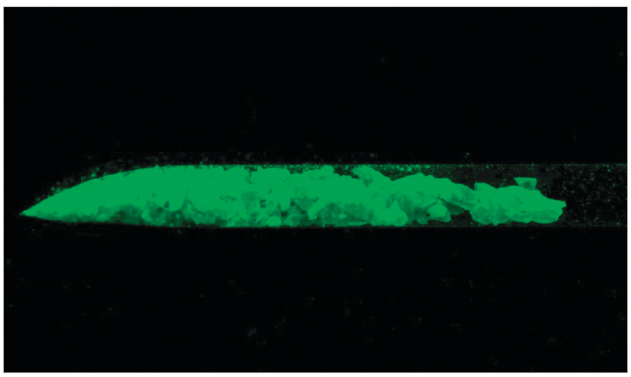

Fig. 6 Luminescence of solid Eu(Tp^{iPr_2})$_2$ (**2**) under UV light.

peaking at 552 nm (18 120 cm^{-1}) can be assigned to the parity-allowed 4f^{6}5d^1 → 4f^7 transition of Eu(II). Its position is in very good agreement with the emissions reported for EuTp$_2$,[22] and Eu(II)-activated nitridosilicates, in which Eu(II) is also coordinated by N-based ligands in its first coordination sphere.[23] A ligand-to-metal charge transfer (LMCT) induced luminescence as suggested for EuTp$_2$[22] is excluded due to the high excitation wavelength of 450 nm (22 220 cm^{-1}) used for the detection of the emission spectrum of Eu(Tp^{iPr_2})$_2$ (**2**). The π → π* transitions of the pyrazole units leading to a LMCT are typically located in the range of 220 nm and thus beyond the range of measureable wavelengths of the used spectrometer.[24]

The photoluminescence excitation spectrum reveals the presence of a raw fine structure that is characteristic for the ^7F_J levels arising from the 4f^6 core of the excited 4f^{6}5d^1 configuration assuming a weak Coulomb interaction between the 4f and 5d electrons and rarely observed.[25] This feature is another evidence for the presence of Eu(II) in the compound and justifies the assignment of the respective emissive transition. Moreover, the emission does not change with different excitation energies (320–480 nm), which is another evidence that the whole excitation band is originated by Eu(II). From the photoluminescence spectra of compound (**2**), the Stokes shift was estimated with 2830 cm^{-1}. Both the Stokes shift and the

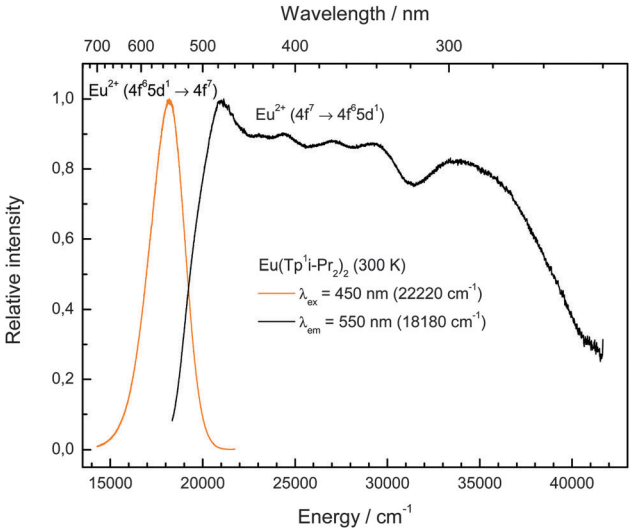

Fig. 7 Room temperature emission (left, yellow line, λ_{ex} = 450 nm) and excitation (right, black line, λ_{em} = 550 nm) spectra of Eu(Tp^{iPr_2})$_2$ (**2**).

FWHM of the emission band are relatively low for a molecular compound and close to values known for Eu(II)-activated ionic compounds.[19] This can be explained by the rigidity of the very bulky tripodal Tp^{iPr_2} ligands that do not allow a large change in metal–ligand distances upon excitation of the complex. An indication that this argument is correct is the even smaller Stokes Shift of Eu(Cp^{BIG})$_2$ (2140 cm^{-1}),[21] where a large degree of rigidity can be assumed too.

3. Conclusions

In summarizing the work reported here, the series of homoleptic lanthanide(II) hydro-tris(pyrazolyl)borate complexes Ln(Tp^{iPr_2})$_2$ (Ln = Sm (**1**), Eu (**2**), Tm (**3**), Yb (**4**); Tp^{iPr_2} = hydro-tris(3,5-diisopropylpyrazolyl)borate) has been completed by the high-yield synthesis of the hitherto unknown europium and ytterbium derivatives **2** and **4**. A single crystal X-ray diffraction study of the ytterbium(II) derivative **4** revealed the same "bent sandwich-like" structure as was previously found for the Sm and Tm compounds **1** and **3**. This finding confirmed that the bent geometry is an inherent structural feature of the Ln(Tp^{iPr_2})$_2$ complexes. An initial reactivity study toward acetonitrile revealed a significant increase in reactivity in the sequence Eu ≈ Yb < Sm < Tm. The Eu (**2**) and Yb (**4**) compounds did not react with acetonitrile even upon heating. The Sm(II) complex **1** afforded the dark green acetonitrile solvate Sm^{II}(Tp^{iPr_2})$_2$·CH$_3$CN (**5**) in addition to the partially ligand fragmented Sm(III) complex, (Tp^{iPr_2})Sm^{III}(3,5-^{i}Pr$_2$pz)$_2$(NCCH$_3$) (**6**). The most reducing thulium(II) complex **3** only yielded ligand fragmented pyrazabole and unidentified Tm(III) species. Despite the opening of the coordination sphere in the "bent sandwich-like" Ln(Tp^{iPr_2})$_2$ complexes, apparently not even rod-like donor ligands such as CH$_3$CN are able to enter the coordination sphere of the central Ln^{2+} ions. Together with the previous studies on the "linear" homoleptic Ln(II) complexes Ln(Tp^{Me_2})$_2$ these results clearly

demonstrate that there is an intricate balance between stability and reactivity of such homoleptic lanthanide(II) tris(pyrazolyl)-borate complexes. While the smaller Tp^{Me_2} provided versatile reactivity to the $Sm(Tp^{Me_2})_2$ complex,[8–11] it could only produce a thermally very sensitive $Tm(Tp^{Me_2})_2$.[14] In contrast, the very bulky Tp^{iPr_2} ligand stabilizes Tm(II), but hinders reactivity. Photoluminescence studies on $Eu(Tp^{iPr_2})_2$ at room temperature revealed an exceptionally intense yellow emission at 552 nm (18 120 cm^{-1}, FWHM = 2245 cm^{-1}, Stokes shift = 2830 cm^{-1}) under excitation at 450 nm that can be assigned to a parity-allowed $4f^6 5d^1 \rightarrow 4f^7$ transition of Eu(II) in the complex, supporting the sole presence of the divalent lanthanide. An intense emission is also observable at sunlight excitation. The luminescence characteristics are comparable to the values known from N-coordinated Eu(II) in ionic compounds, and indicates that the Tp^{iPr_2} ligands provide a rigid coordination environment to the Eu(II) center.

4. Experimental section

4.1 General procedures

All operations were performed with rigorous exclusion of air and water in oven-dried or flame-dried glassware under an inert atmosphere of dry argon, employing standard Schlenk, high-vacuum and glovebox techniques (MBraun MBLab; <1 ppm O_2, <1 ppm H_2O or Vacuum Atmosphere, model HE-553-2). THF, diethyl ether, and *n*-pentane were dried over sodium/benzophenone and freshly distilled under nitrogen atmosphere prior to use. Acetonitrile was dried over calcium hydride. All glassware was oven-dried at 120 °C for at least 24 h, assembled while hot and cooled under high vacuum prior to use. THF solvates of the three lanthanide diiodides, $LnI_2(THF)_2$, were prepared from the rare-earth metal powders and 1,2-diiodoethane in THF according to a well-established method by Kagan.[26] The starting material KTp^{iPr_2} was obtained through a melt reaction between KBH_4 and 3 equiv. of 3,5-diisopropylpyrazole at 260 °C according to the method published by Kitajima *et al.*[13] The NMR spectra were recorded in C_6D_6 or THF-d_8 solutions on a Bruker DPX 600 (^{1}H: 600.1 MHz; ^{13}C: 150.9 MHz) or a Bruker AVANCE III 400 MHz (5 mm BB, ^{1}H: 400.1 MHz; ^{13}C: 100.6 MHz), ^{1}H and ^{13}C shifts are referenced to internal solvent resonances and reported in parts per million relative to TMS. IR (KBr) spectra were measured using a Perkin-Elmer FT-IR 2000 spectrometer. Mass spectra (EI, 70 eV) were run on a MAT 95 apparatus. Microanalyses of the compounds were performed using a Leco CHNS 923 apparatus. Photoluminescence measurements were performed at room temperature on a Fluorolog3 spectrofluorometer FL3-22 from Horiba JobinYvon equipped with double Czerny–Turner monochromators and a 450 W Xe lamp. The emission spectrum was corrected for the photomultiplier sensitivity and the excitation spectrum for the intensity of the excitation source. Measurements were made on crystalline compound **2**, after the solid was sealed in silica ampoules under vacuum.

4.2 Preparation of $Eu(Tp^{iPr_2})_2$ (2)

Solid $EuI_2(THF)_2$ (1.73 g, 3.16 mmol) was added to a stirred solution of KTp^{iPr_2} (3.2 g; 6.33 mmol) in 150 ml of THF. Stirring at r.t. was continued for 24 h to give a ''neon-yellow'', strongly fluorescent solution and a white precipitate (KI). After filtration and evaporation of the clear, yellow filtrate to dryness, the residue was extracted with *n*-pentane (80 ml) and filtered again. The filtrate was concentrated *in vacuo* to a total volume of *ca.* 25 ml. Cooling to −20 °C for 3d produced bright yellow crystals of **2**. Yield: 2.84 g (83%). Decomposition range: 78–84 °C. Anal. calcd for $C_{54}H_{92}B_2EuN_{12}$ (1082.99 g mol^{-1}): C, 59.89; H, 8.56; N, 15.52. Found: C, 59.39; H, 8.31; N, 14.98. IR (KBr): ν_{max} = 3222m, 3103m, 2964vs, 2930s, 2871s, 2552w, 2471w, 2240w, 1959w, 1638m, 1567m, 1535m, 1468s, 1427m, 1381s, 1367s, 1300s, 1235m, 1174s, 1138m, 1105m, 1073m, 1050s, 1009m, 991m, 959w, 924w, 897w, 879w, 791s, 771m, 724m, 717m, 663m cm^{-1}. MS (EI): *m*/*z* 988 (7%), 935 (6, [M − pz^{iPr_2}]), 768 (100, [$Tp^{iPr_2}Eu$ + pz^{iPr_2}]), 616 (88, [$Tp^{iPr_2}Eu$]), 477 (40, [Tp^{iPr_2} + BH]), 302 (23, [pz^{iPr_2}]$_2$). ^{11}B NMR (300 K, C_6D_6, 128 MHz): δ = −7 (v, br).

4.3 Preparation of $Yb(Tp^{iPr_2})_2$ (4)

In a similar manner as described for **2**, the reaction of $YbI_2(THF)_2$ (1.69 g, 2.96 mmol) with KTp^{iPr_2} (3.0 g, 5.93 mmol) in 80 ml THF afforded, after crystallization from *n*-pentane and thorough drying to remove residual *n*-pentane, bright red crystalline **4** in 77% isolated yield (2.51 g). Mp. 99 °C (beginning dec.). Anal. calcd for $C_{54}H_{92}B_2N_{12}Yb$ (1104.07 g mol^{-1}): C, 58.75; H, 8.40; N, 15.22. Found: C, 58.33; H, 8.10; N, 14.88. IR (KBr): ν_{max} = 3222m, 3092m, 2966vs, 2931s, 2870s, 2555m, 2237w, 1959w, 1638s, 1566m, 1538s, 1470s, 1426m, 1381s, 1368s, 1298s, 1237m, 1175s, 1138m, 1106m, 1053s, 1020m, 960w, 924w, 896w, 878w, 794s, 725m, 717m, 661m cm^{-1}. MS (EI): *m*/*z* 996 (7%), 968 (8), 953 (6, [M − pz^{iPr_2}]), 817 (28), 790 (100, [$Tp^{iPr_2}Yb$ + pz^{iPr_2}]), 637 (6, [$Tp^{iPr_2}Eu$]), 476 (9, [Tp^{iPr_2} + BH]), 321 (14, [pz^{iPr_2} + Yb]), 169 (19), 137 (25). ^{1}H NMR (300 K, C_6D_6, 400 MHz): δ = 5.93 (s, 6H, pyrazolyl), 5.22 (s br, 2H, B–*H*), 3.73 (sept, 6H, C–*H* ^{i}Pr, *J* = 6.8 Hz), 2.66 (sept, 6H, C–*H* ^{i}Pr, *J* = 6.8 Hz), 1.22 (d, 36 H, CH_3 ^{i}Pr, *J* = 6.8 Hz), 1.04 (d, 36 H, CH_3 ^{i}Pr, *J* = 6.8 Hz). ^{13}C NMR (300 K, C_6D_6, 100 MHz): δ = 160.6 (q-*C* pyrazolyl), 156.9 (q-*C* pyrazolyl), 97.5 (*C*–H pyrazolyl), 28.0 (*C*–H ^{i}Pr), 27.1 (*C*–H ^{i}Pr), 24.8 (*C*H$_3$ ^{i}Pr), 23.8 (*C*H$_3$ ^{i}Pr). ^{171}Yb (300 K, C_6D_6, 70 MHz, relative to [Yb(η-C_5Me_5)$_2$(THF)$_2$]): δ = 619.1. ^{11}B NMR (300 K, C_6D_6, 128 MHz): δ = −6.2 (s, br).

4.4 Behavior of $Sm(Tp^{iPr_2})_2$ (1) toward acetonitrile

Addition of acetonitrile (2–3 ml) to *ca.* 200 mg of $Sm(Tp^{iPr_2})_2$ (**1**) produced an almost colorless supernatant and a dark green, almost black solid (unchanged Sm(II)). The supernatant was pipetted off and the solid dissolved in Et_2O to give a very dark green solution, to which acetonitrile was again added. An attempt to grow crystals by cooling at −30 °C was unsuccessful. The dark green solution was left to slowly evaporate at RT, and overnight deposited a mixture of dark green and colorless crystals. The supernatant was removed and the mixture of crystals

briefly dried. From this mixture a dark green and a colorless crystal were selected and, by X-ray diffraction, were shown to be complexes **5** and **6**, respectively.

4.5 X-ray crystallographic studies of 4–6

The intensity data of **4** were registered on an Oxford Diffraction Nova A diffractometer using mirror-focussed CuK_α radiation. Absorption correction was applied using the multi-scan method. The structure was solved by direct methods (SHELXS-97)[27a] and refined by full matrix least-squares methods on F^2 using SHELXL-97.[27b] Intensity data for **5** and **6** were collected on a Bruker D8/APEX II CCD diffractometer using graphite-monochromated MoK_α radiation. Programs for diffractometer operation, data collection, data reduction and absorption correction were those supplied by Bruker. Absorption corrections were applied using the Gaussian integration (face-indexed) method. The structures were solved and refined using the programs SHELXT and SHELXL-2013.[28] Data collection parameters for **4–6** are given in Table 1.

Acknowledgements

Financial support by the Otto-von-Guericke-Universität Magdeburg is gratefully acknowledged. JT thanks NSERC and the University of Alberta for financial support. Thanks are due to Ms Desirée Schneider and Dr Volker Lorenz for technical assistance in the preparation of the manuscript.

References

1 Review: F. T. Edelmann, Complexes of Scandium, Yttrium and Lanthanide Elements, in *Comprehensive Organometallic Chemistry III*, ed. R. H. Crabtree and D. M. P. Mingos, Elsevier, Oxford, 2006, p. 1.

2 (*a*) W. J. Evans, L. A. Hughes and T. P. Hanusa, *J. Am. Chem. Soc.*, 1984, **106**, 4270; (*b*) W. J. Evans, J. W. Grate, H. W. Choi, I. Bloom, W. E. Hunter and J. L. Atwood, *J. Am. Chem. Soc.*, 1985, **107**, 941; (*c*) W. J. Evans, L. A. Hughes and T. P. Hanusa, *Organometallics*, 1986, **5**, 1285; (*d*) C. J. Burns and R. A. Andersen, *J. Am. Chem. Soc.*, 1987, **109**, 5853, and references cited therein; (*e*) D. J. Berg, C. J. Burns, R. A. Andersen and A. Zalkin, *Organometallics*, 1989, **8**, 1865; (*f*) W. J. Evans, S. L. Gonzales and J. W. Ziller, *J. Am. Chem. Soc.*, 1991, **113**, 7423, and references cited therein; (*g*) M. Shultz, C. J. Burns, D. J. Schwartz and R. A. Andersen, *Organometallics*, 2000, **19**, 781; (*h*) J. A. Moore, A. H. Cowley and J. C. Gordon, *Organometallics*, 2006, **25**, 5207.

3 W. J. Evans, T. A. Ulibarri and J. W. Ziller, *J. Am. Chem. Soc.*, 1988, **110**, 6877.

4 (*a*) S. N. Konchenko, N. A. Pushkarevsky, M. T. Gamer, R. Köppe, H. Schnöckel and P. W. Roesky, *J. Am. Chem. Soc.*, 2009, **131**, 5740; (*b*) T. Li, M. T. Gamer, M. Scheer, S. N. Konchenko and P. W. Roesky, *Chem. Commun.*, 2013, **49**, 2183; (*c*) N. Arlet, S. Bestgen, M. T. Gamer and P. W. Roesky, *J. Am. Chem. Soc.*, 2014, **136**, 14023.

5 (*a*) R. A. Andersen, J. M. Boncella, C. J. Burns, J. C. Green, D. Hohl and N. Rösch, *J. Chem. Soc., Chem. Commun.*, 1986, 405; (*b*) J. C. Green, D. Hohl and N. Rösch, *Organometallics*, 1987, **6**, 712; (*c*) T. K. Hollis, J. K. Burdett and B. Bosnich, *Organometallics*, 1993, **12**, 3385; (*d*) T. V. Timofeeva, J.-H. Lii and N. L. Allinger, *J. Am. Chem. Soc.*, 1995, **117**, 7452; (*e*) J. Marcalo, A. Pires de Matos and W. J. Evans, *Organometallics*, 1996, **15**, 345; (*f*) L. Perrin, L. Maron, O. Eisenstein, D. J. Schwartz, C. J. Burns and R. A. Anderson, *Organometallics*, 2003, **22**, 5447; (*g*) S. Labouille, C. Clavaguera and F. Nief, *Organometallics*, 2013, **32**, 1265; (*h*) C. E. Kefalidis, S. Essafi, L. Perrin and L. Maron, *Inorg. Chem.*, 2014, **53**, 3427; (*i*) C. E. Kefalidis, L. Perrin, C. J. Burns, D. J. Berg, L. Maron and R. A. Andersen, *Dalton Trans.*, 2015, **44**, 2575.

6 S. Trofimenko, *The Coordination Chemistry of Scorpionates – Pyrazolylborate Ligands*, Imperial College Press, London, 1999.

7 C. Pettinari, *Scorpionates II: Chelating Borate Ligands*, Imperial College Press, London, 2008.

8 J. Takats, X. W. Zhang, V. W. Day and T. A. Eberspacher, *Organometallics*, 1993, **12**, 4286.

9 G. H. Maunder, A. Sella and D. A. Tocher, *J. Chem. Soc., Chem. Commun.*, 1994, 885.

10 A. C. Hillier, X. W. Zhang, G. H. Maunder, S. Y. Liu, T. A. Eberspacher, M. V. Metz, R. McDonald, Â. Domingos, N. Marques, V. W. Day, A. Sella and J. Takats, *Inorg. Chem.*, 2001, **40**, 5106.

11 Review: N. Marques, A. Sella and J. Takats, *Chem. Rev.*, 2002, **102**, 2137.

12 C. E. Davies, I. M. Gardiner, J. C. Green, M. L. H. Green, N. J. Hazel, P. D. Grebenik, V. S. B. Mtetva and K. Prout, *J. Chem. Soc., Dalton Trans.*, 1985, 669.

13 N. Kitajima, K. Fujisawa, C. Fujimoto, Y. Moro-oka, S. Hasimoto, T. Kitagawa, K. Toriumi, K. Tatsumi and A. Nakamura, *J. Am. Chem. Soc.*, 1992, **114**, 1277.

14 A. Momin, L. Carter, Y. Yang, R. McDonald, S. Essafi, F. Nief, I. Del Rosal, A. Sella, L. Maron and J. Takats, *Inorg. Chem.*, 2014, **53**, 12066.

15 (*a*) A. G. Avent, M. A. Edelman, M. F. Lappert and G. A. Lawless, *J. Am. Chem. Soc.*, 1989, **111**, 3423; (*b*) J. M. Keates, G. A. Lawless and M. P. Waugh, *Chem. Commun.*, 1996, 1627; (*c*) J. M. Keates and G. A. Lawless, ^{171}Yb NMR Spectroscopy, in *Advanced Applications of NMR to Organometallic Chemistry*, ed. M. Gielen, R. Willem and B. Wrackmeyer and J. Wiley & Sons, Chichester, 1996, ch. 12, pp. 357–370; (*d*) J. M. Keates and G. A. Lawless, *Organometallics*, 1997, **16**, 2842.

16 (*a*) X. Y. Zhang, R. McDonald and J. Takats, *New J. Chem.*, 1995, **19**, 573; (*b*) P. B. Hitchcock, M. F. Lappert and S. Tian, *Organometallics*, 2000, **19**, 4320; (*c*) K. Izod, P. O'Shaughnessy, J. M. Sheffield, W. Clegg and S. T. Liddle, *Inorg. Chem.*, 2000, **39**, 4741; (*d*) P. B. Hitchcock, M. F. Lappert and S. Prashar, *J. Organomet. Chem.*, 2000, **613**, 105; (*e*) M. Niemeyer, *Eur. J. Inorg. Chem.*, 2001,

1969; (*f*) G. B. Deacon and C. M. Forsyth, *Chem. – Eur. J.*, 2004, **10**, 1798; (*g*) M. Niemeyer, *Inorg. Chem.*, 2006, **45**, 9085; (*h*) L. J. Bowman, K. Izod, W. Clegg and R. W. Harrington, *Organometallics*, 2007, **26**, 2646; (*i*) A. Edelmann, S. Blaurock, V. Lorenz, L. Hilfert and F. T. Edelmann, *Angew. Chem., Int. Ed.*, 2007, **46**, 6732.

17 R. D. Shannon, *Acta Crystallogr., Sect. A: Cryst. Phys., Diffr., Theor. Gen. Crystallogr.*, 1976, **32**, 751.

18 C. Ronda, *Luminescence*, Wiley-VCH, Weinheim, Germany, 2008.

19 W. M. Yen, S. Shionoya and H. Yamamoto, *Phosphor Handbook*, CRC Press, 2007.

20 P. Dorenbos, *J. Lumin.*, 2003, **104**, 239.

21 S. Harder, D. Naglav, C. Ruspic, C. Wickleder, M. Adlung, W. Hermes, M. Eul, R. Pöttgen, D. B. Rego, F. Poineau, K. R. Czerwinski, R. H. Herber and I. Nowik, *Chem. – Eur. J.*, 2013, **37**, 12272.

22 C. P. Shipley, S. Capecchi, O. V. Salata, M. Etchells, P. J. Dobson and V. Christou, *Adv. Mater.*, 1999, **11**, 533.

23 (*a*) Y. Q. Li, J. E. J. V. Steen, J. W. H. V. Krevel, G. Botty, A. C. Delsing, F. J. DiSalvo, G. D. With and H. T. Hintzen, *J. Alloys Compd.*, 2006, **417**, 273; (*b*) H. A. Höppe, H. Lutz, P. Morys, W. Schnick and A. Seilmeier, *J. Phys. Chem. Solids*, 2000, **61**, 2001; (*c*) V. Bachmann, C. Ronda, O. Oeckler, W. Schnick and A. Meijerink, *Chem. Mater.*, 2009, **21**, 316.

24 D. S. Noyce, E. Ryder and B. H. Walker, *J. Org. Chem.*, 1955, **20**, 1681.

25 (*a*) S. H. M. Poort, J. W. H. van Krevel, R. Stomphorst, A. P. Vink and G. Blasse, *J. Solid State Chem.*, 1996, **122**, 432; (*b*) A. Meijerink and G. Blasse, *J. Lumin.*, 1989, **43**, 283; (*c*) M. Suta, P. Larsen, F. Lavoie-Cardinal and C. Wickleder, *J. Lumin.*, 2014, **149**, 35.

26 J. L. Namy, H. B. Kagan and P. E. Caro, *New J. Chem.*, 1981, **5**, 479.

27 (*a*) G. M. Sheldrick, *SHELXL-97 Program for Crystal Structure Refinement*, Universität Göttingen, Germany, 1997; (*b*) G. M. Sheldrick, *SHELXS-97 Program for Crystal Structure Solution*, Universität Göttingen, Germany, 1997.

28 G. M. Sheldrick, *Acta Crystallogr., Sect. A: Found. Crystallogr.*, 2008, **64**, 112.